Research Article

Journal of Environmental Nanotechnology

Neural Network-based Prediction and Optimization of Performance in Single Slope Solar Stills Enhanced with Nanoparticles for Improved Water Production

D. Nisha[1*], V. Stanlin Prija[2], W. V. Sherlin Sherly[3] and P. Girija[2]

[1]Department of Information Technology, SRM Valliammai Engineering College, Kattankulathur, TN, India
[2]Department of Computer Science and Engineering, Vel Tech High Tech Dr. Rangarajan Dr.Sakunthala Engineering College, Chennai, TN, India
[3]Department of Artificial Intelligence & Data Science, Jeppiaar Institute of Technology, Kunnam, Sunguvarchathram, Chennai, TN, India
Received: 19.09.2024 Accepted: 25.12.2024 Published: 30.12.2024
*davidnisha21@gmail.com

ABSTRACT

This research uses a neural network technique to anticipate and optimize temperature and production factors in a single-slope solar still. In addition to comparable productivity measures and actual and expected temperatures of the glass and water, the experimental dataset contains changes in sun intensity, water depth, and the proportion and type of nanoparticles (TiO_2 and CuO). The goal is to enhance the knowledge and performance of solar stills essential to sustainable freshwater production. Based on input characteristics, a neural network model was developed to forecast water temperature, glass temperature, and Productivity. By contrasting expected results with actual measurements, the model's performance was assessed and shown to have good predictive capabilities. The results showed that the kind and concentration of nanoparticles and sun intensity substantially impacted thermal behavior and Productivity. Productivity levels, for example, varied greatly, from as low as 0.3 kg/m²h with CuO nanoparticles to 2.75 kg/m²h with TiO_2 under some circumstances. RNN, LSTM, and CNN models were tested, with RNN consistently providing the most accurate predictions across all datasets, particularly for Productivity, glass temperature, and water temperature. Along with precise forecasts, optimization methods were used to identify the ideal operating settings for optimum output. This method promotes more effective and environmentally friendly desalination solutions by offering insight into solar still design and operation enhancements. The results may guide future experimental configurations and practical applications for increased water production.

Keywords: Neural network; Solar still; Productivity; Nanoparticles; Optimization; RNN; LSTM; CNN.

1. INTRODUCTION

Neural network models have become very effective tools for forecasting and maximizing the performance of single-slope solar stills essential for sustainable freshwater production. The main goal of this study is to analyze the effects of sun intensity, water depth, and nanoparticles on the thermal behavior and output of solar stills. The paper proposes ideal circumstances for optimizing water production and emphasizes the higher predictive power of RNN models.

Moustafa *et al.* (2022) Studies have demonstrated that adding an electrical heater run by solar photovoltaic panels significantly increased tubular solar stills' thermal efficiency and water production. Furthermore, it has been shown that using the humpback whale optimizer to improve conventional artificial neural network models produces better prediction accuracy than solo models and models optimized using particle swarm techniques.Nazari *et al.* (2020), the performance of solar stills has been modeled by recent research utilizing artificial neural networks, emphasizing variables like water productivity, energy efficiency, and exergy efficiency. It has been shown that integrating optimization methods, including the Imperialist Competition Algorithm, dramatically improves the predictive accuracy of ANN models, increasing the effectiveness of forecasts about the performance of solar stills (Sharshir *et al.* 2022). Recent studies have investigated using innovative materials, such as cobalt oxide nanoparticles and linen wicks, to enhance water evaporation and production rates and to improve the performance of stepped double-slope solar stills. Deep neural networks and other machine learning models have also been used to forecast the performance of solar stills; these models have shown better accuracy than previous methods like decision trees and support vector regression.

Essa *et al.* (2020) new methods such as the Harris Hawks Optimizer, which simulates natural hunting behaviour to adjust model parameters, have been utilized to optimize artificial neural networks in recent advances in solar still production prediction. The Harris Hawk's optimizer dramatically improves prediction accuracy compared to more conventional models like support vector machines and regular neural networks, particularly for active solar stills connected with other systems like condensers.Abdullah *et al.* (2024) a viable

substitute for conventional experimental methods, which are sometimes expensive and time-consuming, is incorporating artificial intelligence techniques in solar still performance prediction, as highlighted in recent work. Numerous machine learning techniques have been investigated to forecast the performance of solar stills, emphasizing their fundamental ideas, benefits, drawbacks, and accuracy as measured by metrics such as root mean square error.Elsheikh *et al*. (2021) long short-term memory (LSTM) neural networks have been used in recent research to estimate the freshwater production of solar stills, showing better forecasting accuracy than more conventional techniques such as autoregressive integrated moving averages. Compared to traditional solar stills, it has been demonstrated that sophisticated designs, such as copper corrugated absorber plates in stepped solar stills, significantly improve thermal performance and water production(Victor *et al*. 2022). Recent research has concentrated on improving solar still performance by utilizing cutting-edge machine learning approaches, including particle swarm optimization and deep neural networks, to increase water production. It has been shown that using innovative designs, such as spiral and straight tube solar water collectors, enhances the effectiveness of solar stills in desalination procedures; studies reveal significant gains in performance when compared to traditional techniques.

Yuvaperiyasamy *et al*. (2023) examined how adding fins and sun ponds to single basin solar stills (SBSS) may improve their thermal efficiency and increase their daily water collection. According to experimental findings, adding fins and finned ponds to solar stills may increase water output by up to 52% compared to traditional SBSS (Senthilkumar *et al*. 2024). Particle swarm optimizationand fuzzy logic interfaces have been used in this research to improve solar still parameters, emphasizing phase transition materials such as silver nanoparticles in paraffin wax and environmental factors. Under various circumstances, the Productivity of pyramid solar stills has been increased by integrating TOPSIS and Taguchi's L_9 orthogonal array.

Migaybil and Gopaluni (2024) suggested that transfer learning may improve the prediction accuracy of solar desalination models, particularly when ANN regression is used to anticipate water production. Comparative studies demonstrate that pre-trained ANN models perform better than conventional models like MLR, exhibiting lower residuals and increased forecast reliability for freshwater production in solar stills.

Mashaly and Alazba (2016) have shown that solar still output can be accurately predicted by artificial neural networks, with models that include operational and climatic factors showing exceptionally high accuracy. When it comes to solar still desalination of agricultural drainage water (ADW), a comparative study shows that ANN works better than multiple linear regression (MLR), with a coefficient of determination above 0.96 and relative errors within ±10%. The efficiency of combining multi-layer perceptions with sophisticated optimization algorithms for forecasting solar still production has been shown byAlsaiari *et al*. (2023). The MLP-ARO model had much-reduced root mean square deviation values across several solar still designs, demonstrating improved accuracy in research comparing MLP models optimized using gradient descent, PSO, GA, and an artificial rabbit's optimizer.

Abujazar *et al*. (2018)have shown that cascaded forward neural networks are more successful than linear and standard regression models for forecasting the Productivity of stepped solar still systems. Assessments of statistical metrics including RMSE, MAPE, and MBE confirm the increased accuracy of CFNN models in simulating solar still performance.Shanmugan *et al*. (2024)acknowledged that combining solar photovoltaic (PV) technology with solar stills successfully increases freshwater output by using both thermal and electrical energy for improved condensation and evaporation processes. According to research, integrating solar PV helps achieve national development goals by addressing water constraints and fostering sustainable energy production.

Hemmat Esfe *et al*. (2021)have investigated using thermoelectric cooling devices to improve single-slope solar stills, demonstrating significant gains in freshwater output. The possibility of geometric optimization and TEC integration for increased efficiency is shown by simulations that show that integrating a TEC system may enhance the freshwater production rate by 6.8%. Still, a 50% increase in length lowers output by around 10%.Alwan *et al*. (2024)despite being a sustainable technique for desalinating brackish water, research has shown that solar distillation has productivity issues. It has been discovered that several design changes, including varying the water depth, the thickness of the glass cover, and adding devices like a revolving drum, significantly improve the performance of solar stills and may increase water output by 200–300%.

According to experimental research, Yuvaperiyasamy *et al*. (2023), including circular fins, water depth, and intake temperature all significantly impact freshwater production in pyramid solar stills. The findings showed that adding fins and raising the water depth and temperature significantly increased freshwater output; the most significant rise was seen at a water depth of 2 cm and an input temperature of 50ºC.Based on study

findings, Yuvaperiyasamy *et al*. (2023), adjusting operating factors such as insulation thickness, depth, water intake temperature, and solar intensity may maximize the output of pyramid solar stills (PSS). The efficiency of response surface methodology and artificial neural networks in determining perfect conditions is confirmed by comparative research; ideal parameters may yield up to 2.585 kg/m² of distillate.Sharon *et al*. (2020)researched solar stills' structure and operational characteristics, emphasizing the importance of components like storage tanks, thermometers, and piping networks in optimizing performance. Their study highlighted design modifications improving solar absorption and thermal efficiency in still setups.They explored enhancements in solar still efficiency, mainly focusing on insulating materials like sawdust to reduce heat loss. Their work demonstrated how strategic design choices, such as insulation and surface treatments, can significantly boost solar stills' thermal performance and water productivity.

The collective literature shows significant advancements in enhancing solar still performance through various design modifications, machine learning models, and integration of novel materials and optimization techniques. Notably, studies highlight the effectiveness of innovative insulation and structural designs in boosting thermal efficiency and freshwater output. Despite these developments, a clear research gap remains in the comprehensive application of neural network-based predictive models, such as RNNs, in conjunction with advanced materials like nanoparticles, to optimize solar still performance under varied environmental conditions. The present experimental study aims to bridge this gap by leveraging a neural network model to analyze the impact of sun intensity, water depth, and nanoparticles (e.g., TiO_2 and CuO) on single-slope solar stills' thermal behavior and Productivity. This approach demonstrates the predictive power and optimization capabilities of RNNs over traditional methods and provides practical insights into achieving sustainable freshwater production with enhanced operational efficiency.

2. MATERIALS AND METHOD

The study outlines the design and components of a typical single-basin solar still (SBSS), highlighting key structural and functional aspects. The SBSS includes a storage tank, solar still, thermometers, and a piping network, forming part of a conservative solar still (Sharon *et al*. 2020). The basin, made from 2 mm thick galvanized iron and 0.12 m deep, is painted matte black to maximize solar absorption, enhancing thermal efficiency. This basin is housed in a wooden box with external dimensions of 1.2 m x 1.2 m and a thickness of 0.19 m, while the height measures 0.1 m. The box's interior is painted white to optimize sunlight reflection onto the water's surface, boosting energy absorption. The experimental setup is shown in Fig. 1. Insulating sawdust is placed between the basin and the wooden crate to minimize heat loss (Mustafa *et al*., 2020). The setup is tested in Coimbatore (latitude 10.9729° N, longitude 77.3698° E), with a 10° angled placement of a plain 5 mm thick glass cover on top to capture sunlight effectively. For added protection against elements such as rain and direct sun radiation, sheet metal encloses all five sides of the wooden crate, ensuring the integrity of the setup during the experiment.

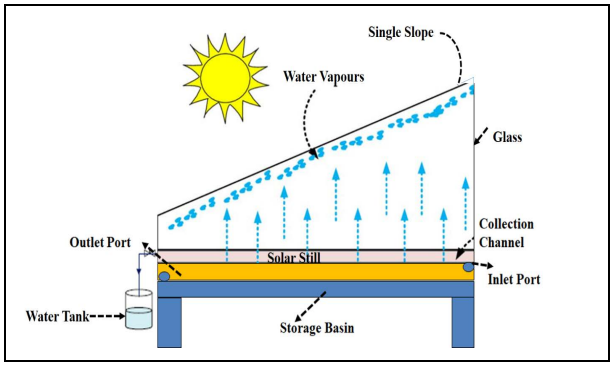

Fig. 1: SBSS experimental design setup image

3. RESULTS AND DISCUSSION

Data from 36 trials that looked at how temperature and Productivity were affected by solar intensity, water depth, and nanoparticle type are shown in Table 1. The water depth ranged from 4 to 8 meters, and the solar intensity ranged from 300 to 900 W/m². TiO_2 and CuO were the most common nanoparticles utilized, with concentrations ranging from 1% to 2%. When comparing actual and expected productivity numbers, the table demonstrates that, on average, the actual outcomes roughly match the projections. Additionally, it compares actual and anticipated temperatures under various experimental situations by measuring the temperatures of glass and water. Significant findings indicate that while water temperature estimates are constant across all tests, higher solar intensity and higher nanoparticle concentrations typically lead to higher productivity and glass temperatures. The information demonstrates how these elements affect the system's Productivity and thermal performance.

The dataset includes several essential input characteristics essential to comprehending experimental settings. First, "Solar Intensity" provides information about the external factors affecting the process by measuring the amount of sun energy received throughout the experiment. "Water Depth" describes the vertical distance between the water's surface and bottom, a critical component influencing several aquatic processes. "% of Nano Particle," another essential parameter,

measures the concentration of nanoparticles used in the experiment and offers vital details on the makeup of the experimental apparatus. Last but not least, the "Type of Nano Particle" feature identifies the particular kind of nanoparticles used, such as CuO (copper oxide) or TiO_2 (titanium dioxide), illuminating the unique traits and attributes of the nanoparticles being studied. When combined, these characteristics provide a thorough comprehension of the experimental design and its underlying factors. Table 2 below shows the pseudocode for the prediction of SBSS performance.

Table 1. Single slope solar still experimental inputs and Output performance

Run	Solar intensity	Water depth	% of nanoparticle	Type of nanoparticle	Productivity		Glass temperature		water temperature	
					Actual	predicted	Actual	predicted	Actual	predicted
1	300	4	1	TiO_2	0.755	0.6943	51.96	52.03	58.26	58.25
2	600	6	1.5	TiO_2	0.987	0.9468	51.68	51.7	57.98	57.93
3	900	8	2	TiO_2	2.12	2.14	57.94	58.07	61.5	61.53
4	300	4	1	TiO_2	0.65	0.6943	52.04	52.03	58.34	58.25
5	600	6	1.5	TiO_2	0.897	0.9468	51.8	51.7	58.11	57.93
6	900	8	2	TiO_2	2.15	2.14	58.28	58.07	61.58	61.53
7	300	4	2	TiO_2	0.55	0.5225	51.58	51.6	57.88	58.01
8	600	6	1	TiO_2	2.32	2.21	54.76	54.67	61	61
9	900	8	1.5	TiO_2	1.49	1.51	53.15	53.42	59.45	59.43
10	300	4	1.5	TiO_2	1.53	1.52	51.23	50.89	59.89	59.8
11	600	6	2	TiO_2	1.45	1.4	52.16	52.05	58	58
12	900	8	1	TiO_2	1.45	1.4	52.6	52.52	58.9	58.88
13	300	6	1	TiO_2	1.16	1.23	52.08	52.07	59	59.02
14	600	8	1.5	TiO_2	1.12	1.19	52.11	51.7	59.1	59.36
15	900	4	2	TiO_2	2.1	2.13	52.82	52.81	57.12	57.15
16	300	6	1.5	TiO_2	1.45	1.48	50.99	51.5	59.9	59.99
17	600	8	2	TiO_2	0.95	0.9155	53.21	53.39	59.5	59.35
18	900	4	1	TiO_2	2.22	2.26	58.96	59.11	61.26	61.34
19	300	6	2	CuO	0.3	0.3681	52.55	52.55	57.35	57.45
20	600	8	1	CuO	0.45	0.5239	50.78	50.96	58.1	57.97
21	900	4	1.5	CuO	2.75	2.7	56.68	56.7	61.1	61.06
22	300	6	2	CuO	0.39	0.3485	51.91	51.87	58.21	57.99
23	600	8	1	CuO	1.06	1.05	51.58	51.72	57.88	57.9
24	900	4	1.5	CuO	2.34	2.32	54.24	54.15	60.94	60.7
25	300	8	1	CuO	0.55	0.4553	51.54	51.21	56.55	56.47
26	600	4	1.5	CuO	1.51	1.45	51.56	51.37	57.86	57.78
27	900	6	2	CuO	0.784	0.7898	52.86	52.88	57.16	57.29
28	300	8	1.5	CuO	0.75	0.8711	51.29	51.62	58.46	58.85
29	600	4	2	CuO	1.02	1.09	47.88	48.21	55.18	55.32
30	900	6	1	CuO	0.589	0.5651	52.65	52.56	58.85	58.79
31	300	8	2	CuO	0.4	0.3584	49.72	49.46	57	56.94
32	600	4	1	CuO	0.598	0.6315	51.87	51.99	57.97	58.22
33	900	6	1.5	CuO	1.32	1.26	55.32	55.25	60.5	60.63
34	300	8	1.5	CuO	0.3	0.2356	51.67	51.72	57.9	57.72
35	600	4	2	CuO	1.1	1.1	52.28	52.21	58.5	58.42
36	900	6	1	CuO	1.78	1.87	58.11	58.07	61.23	61.26

Table 2. Pseudocode of neural networks analysis

	Pseudocode
1.	Define the data - data: numpy array with input features and target values
2.	Separate features and target variable - X: features (all columns except the last) - y: target variable (last column)
3.	Standardize features - scaler = StandardScaler() - X_scaled = scaler.fit_transform(X)
4.	Define RNN model - model_rnn: Sequential model with SimpleRNN, Dense layers - Compile model_rnn with Adam optimizer and mean squared error loss
5.	Define LSTM model - model_lstm: Sequential model with LSTM, Dense layers - Compile model_lstm with Adam optimizer and mean squared error loss
6.	Define CNN model - Reshape X_scaled for CNN input - model_cnn: Sequential model with Conv1D, MaxPooling1D, Flatten, Dense layers - Compile model_cnn with Adam optimizer and mean squared error loss
7.	Train models - Train model_rnn with X_scaled and y for 200 epochs - Train model_lstm with X_scaled and y for 100 epochs - Train model_cnn with reshaped X_scaled and y for 100 epochs
8.	Make predictions - predictions_rnn = model_rnn.predict(X_scaled) - predictions_lstm = model_lstm.predict(X_scaled) - predictions_cnn = model_cnn.predict(reshaped X_scaled)
9.	Print predictions for each input pair - For each model, iterate over predictions and print Productivity for each input pair

The 3D scatter plot in Fig. 2 visualizes the relationship between solar intensity, water depth, and the percentage of nanoparticles (TiO_2 and CuO) in a solar-based system (SBSS). Each point represents a combination of these parameters, with color differentiating between TiO_2 (blue) and CuO (red). It helps identify trends or variations in performance across the parameter space.

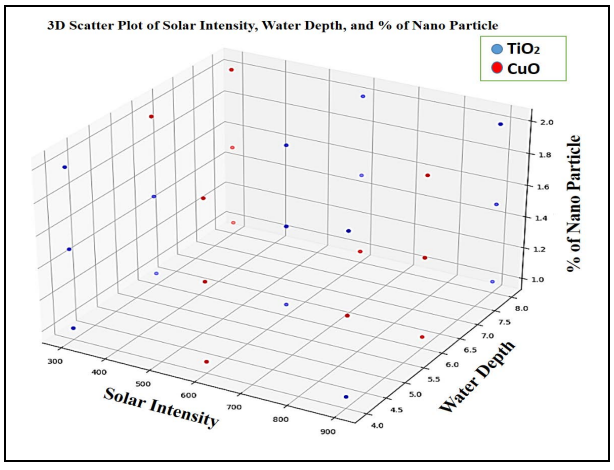

Fig. 2: 3D Scatter plot of SBSS output Performance

3.1 Productivity

The forecasts of the RSM, ANN, RNN, LSTM, and CNN machine learning models and actual productivity levels are contrasted in Table 3. Although the accuracy of each model's predictions varied, the actual productivity numbers ranged from 0.3 to 2.75. With only little variations seen, RSM and ANN forecasts are consistently the ones that are closest to the exact values. However, when LSTM predictions diverge significantly from actual outcomes in severe situations, models like CNN, RNN, and LSTM exhibit more notable variances. Compared to the other models, RSM and ANN provide the most accurate forecasts with fewer mistakes. The table illustrates how well these models predict Productivity in experimental settings when variables like sun intensity and nanoparticle concentration are present. According to these results, RSM and ANN are the most dependable models for this prediction, whereas other models show more output variability.

The MAE and MSE for CNN, LSTM, and RNN models are shown in Table 4, along with their respective dataset performances. With an MAE peaking at only 0.03 and a continuously low error rate, the RNN model may be underfitting because of its low variability. With MAE ranging from 0.01 to 1.33 and MSE from 0.02 to 1.76, the LSTM exhibits more fluctuation, demonstrating its capacity to identify intricate patterns while having more significant peak errors. The CNN often maintains steady performance with an MAE between 0.01 and 0.86 and an MSE up to 0.74, indicating constant but modest error levels. In contrast to RNN's consistent low-error trend, LSTM and CNN exhibit variations despite their sporadic correctness. CNN balances accuracy and stability, whereas LSTM better captures temporal correlations at the occasional expense of significant mistakes.

Fig. 3 compares predicted productivity values by RNN, LSTM, and CNN models with experimental data across 36 runs. The RNN model (orange line) closely follows the actual values (blue line) with minimal deviation, indicating high predictive accuracy. The LSTM (green line) shows more considerable variations, especially in runs with lower Productivity, while the CNN (red line) generally aligns better but shows moderate divergence. Overall, the RNN provides the closest match to experimental values.

The bar chart, Fig. 4, illustrates MAE and MSE for RNN, LSTM, and CNN models in predicting Productivity. The RNN model shows the highest accuracy with the lowest average MAE (0.01) and MSE (0.00), indicating superior predictive performance. The LSTM model performs the weakest, with the most significant average errors (MAE: 0.25, MSE: 0.06). The CNN model ranks between, presenting moderate errors (MAE: 0.26, MSE: 0.07).

Table 3. Productivity output actual vs ANN predicted

Productivity				
Actual	Prediction			
	RSM	ANN		
		RNN	LSTM	CNN
0.755	0.6943	0.7564	1.0184	0.946
0.987	0.9468	0.9912	1.2633	0.9985
2.12	2.14	2.117	1.8749	1.8557
0.65	0.6943	0.6604	1.0184	0.946
0.897	0.9468	0.8912	1.2633	0.9985
2.15	2.14	2.14	1.8749	1.8557
0.55	0.5225	0.5429	1.1883	0.7193
2.32	2.21	2.3277	1.3659	1.4571
1.49	1.51	1.5032	1.9206	1.3623
1.53	1.52	1.5332	1.1026	0.9615
1.45	1.4	1.4568	1.2573	0.9364
1.45	1.4	1.4351	2.0821	1.5923
1.16	1.23	1.1554	1.1737	1.4164
1.12	1.19	1.1364	1.4783	1.3868
2.1	2.13	2.1245	1.7749	1.271
1.45	1.48	1.4376	1.1969	1.1324
0.95	0.9155	0.9506	1.4732	1.5185
2.22	2.26	2.2205	1.9244	2.1846
0.3	0.3681	0.3105	0.7994	0.3626
0.45	0.5239	0.4527	1.2243	0.921
2.75	2.7	2.7461	1.4231	2.3141
0.39	0.3485	0.4075	0.7994	0.3626
1.06	1.05	1.0627	1.2243	0.921
2.34	2.32	2.3361	1.4231	2.3141
0.55	0.4553	0.5662	1.1082	1.2076
1.51	1.45	1.5148	0.9436	1.4992
0.784	0.7898	0.7873	1.2263	0.7584
0.75	0.8711	0.7599	0.9649	0.6685
1.02	1.09	1.0371	0.8854	1.0357
0.589	0.5651	0.5908	1.4405	1.334
0.4	0.3584	0.4161	0.9109	0.4565
0.598	0.6315	0.6049	1.0281	1.0936
1.32	1.26	1.346	1.3104	1.3773
0.3	0.2356	0.3099	0.9649	0.6685
1.1	1.1	1.1071	0.8854	1.0357
1.78	1.87	1.7908	1.4405	1.334

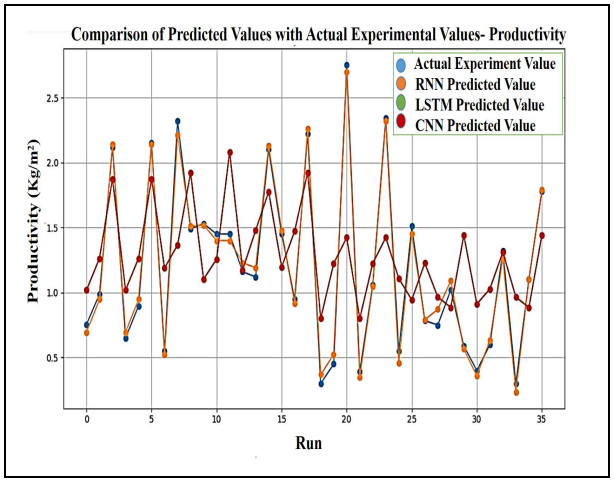

Fig. 3: Comparison of predicted vs actual values of Productivity

The analysis also examined the influence of nanoparticle type and solar intensity on Productivity, which ranged from 0.3 kg/m²h with CuO to 2.75 kg/m²·h with TiO_2. This modeling approach, paired with optimization, helps enhance solar still designs for better desalination outcomes.

Table 4. ANN Performance metric of Productivity

ANN Performance Metric					
RNN		LSTM		CNN	
MAE	MSE	MAE	MSE	MAE	MSE
0	0	0.26	0.07	0.19	0.04
0	0	0.28	0.08	0.01	0
0	0	0.25	0.06	0.26	0.07
0.01	0	0.37	0.14	0.3	0.09
0.01	0	0.37	0.13	0.1	0.01
0.01	0	0.28	0.08	0.29	0.09
0.01	0	0.64	0.41	0.17	0.03
0.01	0	0.95	0.91	0.86	0.74
0.01	0	0.43	0.19	0.13	0.02
0	0	0.43	0.18	0.57	0.32
0.01	0	0.19	0.04	0.51	0.26
0.01	0	0.63	0.4	0.14	0.02
0	0	0.01	0	0.26	0.07
0.02	0	0.36	0.13	0.27	0.07
0.02	0	0.33	0.11	0.83	0.69
0.01	0	0.25	0.06	0.32	0.1
0	0	0.52	0.27	0.57	0.32
0	0	0.3	0.09	0.04	0
0.01	0	0.5	0.25	0.06	0
0	0	0.77	0.6	0.47	0.22
0	0	1.33	1.76	0.44	0.19
0.02	0	0.41	0.17	0.03	0
0	0	0.16	0.03	0.14	0.02
0	0	0.92	0.84	0.03	0
0.02	0	0.56	0.31	0.66	0.43
0	0	0.57	0.32	0.01	0
0	0	0.44	0.2	0.03	0
0.01	0	0.21	0.05	0.08	0.01
0.02	0	0.13	0.02	0.02	0
0	0	0.85	0.73	0.75	0.56
0.02	0	0.51	0.26	0.06	0
0.01	0	0.43	0.18	0.5	0.25
0.03	0	0.01	0	0.06	0
0.01	0	0.66	0.44	0.37	0.14
0.01	0	0.21	0.05	0.06	0
0.01	0	0.34	0.12	0.45	0.2

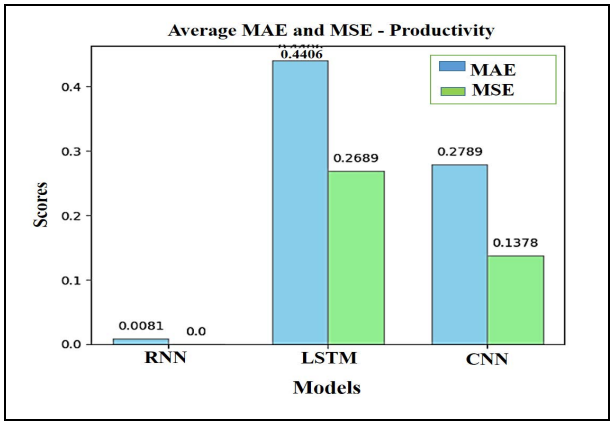

Fig. 4: MAE and MSE value measure of Productivity

3.2 Glass Temperature

Table 5 presents the actual glass temperature values alongside predictions made using different modeling techniques: Response Surface Methodology (RSM), Artificial Neural Network (ANN), Recurrent

Neural Network (RNN), Long Short-Term Memory (LSTM), and Convolutional Neural Network (CNN). The actual temperatures are compared with the predicted values for each model to evaluate the prediction accuracy. The models show varying levels of accuracy, with RSM and ANN predictions generally closest to the actual values. However, the LSTM and CNN models sometimes produce more divergent results.

Table 5. Glass temperature output actual vs ANN predicted

Glass Temperature				
Actual	Prediction			
	RSM	ANN		
		RNN	LSTM	CNN
51.96	52.03	52.0055	55.3476	52.4998
51.68	51.7	51.59	49.1985	39.8902
57.94	58.07	57.8649	53.428	51.2086
52.04	52.03	52.0255	55.3476	52.4998
51.8	51.7	51.59	49.1985	39.8902
58.28	58.07	58.4649	53.428	51.2086
51.58	51.6	50.7655	52.1521	59.9527
54.76	54.67	54.2482	50.8461	45.3572
53.15	53.42	53.4613	54.8917	40.0087
51.23	50.89	51.1953	53.6594	47.7526
52.16	52.05	52.1748	69.0659	73.6241
52.6	52.52	52.6059	56.5558	47.5338
52.08	52.07	52.0663	54.9551	53.4753
52.11	51.7	52.0672	48.8944	37.7137
52.82	52.81	52.7481	54.0959	56.9486
50.99	51.5	51.0008	53.2737	46.8262
53.21	53.39	53.2412	47.4785	51.6478
58.96	59.11	58.8895	57.2503	50.7224
52.55	52.55	52.5933	51.7663	48.8491
50.78	50.96	50.9177	50.5434	64.6324
56.68	56.7	56.5988	55.6231	47.2119
51.91	51.87	51.7933	51.7663	48.8491
51.58	51.72	51.6477	50.5434	64.6324
54.24	54.15	54.1188	55.6231	47.2119
51.54	51.21	51.4381	54.6487	70.6781
51.56	51.37	51.5778	49.5133	42.0834
52.86	52.88	52.8431	53.7485	44.384
51.29	51.62	51.3136	52.9391	48.9659
47.88	48.21	47.8493	48.0355	44.0644
52.65	52.56	52.6849	56.9635	63.8861
49.72	49.46	49.6711	51.4167	47.6364
51.87	51.99	51.8381	51.2047	65.9582
55.32	55.25	55.3424	55.2596	44.2316
51.67	51.72	51.7136	52.9391	48.9659
52.28	52.21	52.2693	48.0355	44.0644
58.11	58.07	58.1149	56.9635	63.8861

Table 6 presents the actual glass temperature values alongside predictions made using different modeling techniques: Response Surface Methodology (RSM), Artificial Neural Network (ANN), Recurrent Neural Network (RNN), Long Short-Term Memory (LSTM), and Convolutional Neural Network (CNN). The actual temperatures are compared with the predicted values for each model to evaluate the prediction accuracy. The models show varying levels of accuracy, with RSM and ANN predictions generally closest to the actual values. However, the LSTM and CNN models sometimes produce more divergent results.

Table 6. ANN Performance metric of glass temperature

ANN Performance Metric					
RNN		LSTM		CNN	
MAE	MSE	MAE	MSE	MAE	MSE
0.05	0	3.39	11.48	0.54	0.29
0.09	0.01	2.48	6.16	11.79	139
0.08	0.01	4.51	20.36	6.73	45.31
0.01	0	3.31	10.94	0.46	0.21
0.21	0.04	2.6	6.77	11.91	141.84
0.18	0.03	4.85	23.54	7.07	50
0.81	0.66	0.57	0.33	8.37	70.1
0.51	0.26	3.91	15.32	9.4	88.41
0.31	0.1	1.74	3.03	13.14	172.69
0.03	0	2.43	5.9	3.48	12.09
0.01	0	16.91	285.81	21.46	460.71
0.01	0	3.96	15.65	5.07	25.67
0.01	0	2.88	8.27	1.4	1.95
0.04	0	3.22	10.34	14.4	207.25
0.07	0.01	1.28	1.63	4.13	17.05
0.01	0	2.28	5.22	4.16	17.34
0.03	0	5.73	32.85	1.56	2.44
0.07	0	1.71	2.92	8.24	67.86
0.04	0	0.78	0.61	3.7	13.7
0.14	0.02	0.24	0.06	13.85	191.89
0.08	0.01	1.06	1.12	9.47	89.64
0.12	0.01	0.14	0.02	3.06	9.37
0.07	0	1.04	1.07	13.05	170.37
0.12	0.01	1.38	1.91	7.03	49.39
0.1	0.01	3.11	9.66	19.14	366.27
0.02	0	2.05	4.19	9.48	89.81
0.02	0	0.89	0.79	8.48	71.84
0.02	0	1.65	2.72	2.32	5.4
0.03	0	0.16	0.02	3.82	14.56
0.03	0	4.31	18.61	11.24	126.25
0.05	0	1.7	2.88	2.08	4.34
0.03	0	0.67	0.44	14.09	198.48
0.02	0	0.06	0	11.09	122.95
0.04	0	1.27	1.61	2.7	7.31
0.01	0	4.24	18.02	8.22	67.5
0	0	1.15	1.31	5.78	33.36

The Fig.5 presents a comparative analysis of actual and predicted glass temperatures across different runs. The experimental values are shown in blue, while the predicted values from RNN, LSTM and CNN models are represented in green, orange, and red respectively. The plot demonstrates how closely each model's predictions align with the actual values, with CNN showing the most variation from the actual data. The fluctuations highlight the models' different levels of accuracy.Based on average values, the RNN model performs better than the other two models, according to the performance measures for the three models: CNN, LSTM, and RNN. In particular, the RNN produces the most accurate forecasts with the least amount of departure from the actual values, with the lowest average mean squared error of 4.91 and mean absolute error of 0.09. The MAE and MSE values of the CNN and LSTM models are much more significant in contrast; the CNN model has an average MAE of 6.34 and MSE of 85.34, while the LSTM model has an average MAE of 3.01 and MSE of 47.47. As a result, with its greater predicted accuracy, the RNN model performs the best on this dataset.

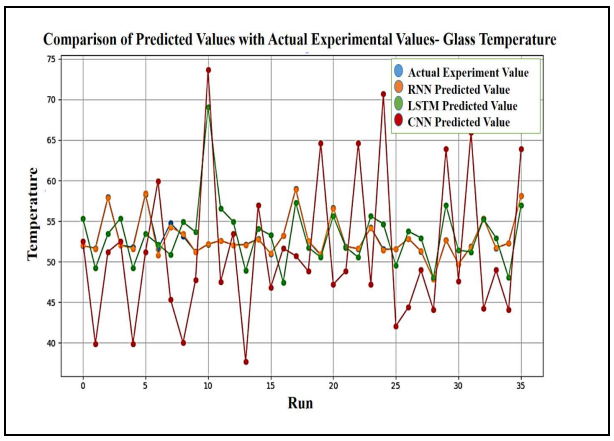

Fig. 5: Comparison of predicted vs actual values of glass temperature

The bar graph Fig. 6 shows how well three models RNN, LSTM, and CNN perform in forecasting glass temperature using the MAE and MSE measures. RNN performs the best, as demonstrated by its lowest MAE (0.0926) and MSE (0.0311). CNN has the highest numbers, with an MAE of 7.8308 and a substantial MSE of 87.5733, whereas LSTM has a greater MAE of 2.6017 and MSE of 14.7656. This implies that RNN is the most accurate of the three models for this research study.

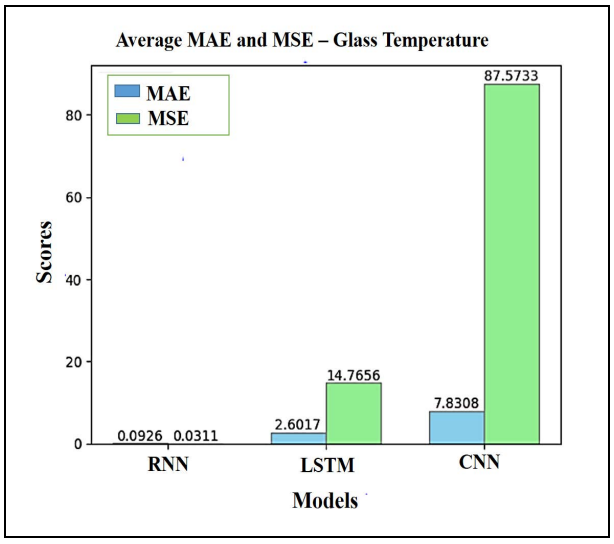

Fig. 6: MAE and MSE value measure of glass temperature

3.3 Water Temperature

Table 7 shows forecasts from many ANN-RNN, LSTM, and CNN models in addition to real water temperature observations. Every row compares the actual and anticipated values for a distinct observation. CNN projections often differ more than RNN predictions, which are more in line with the actual temperatures. This implies that, in comparison to the other models, RNN anticipates water temperature more accurately.

Table 7. Water temp. output actual vs ANN predicted

Actual	Prediction			
	RSM	ANN		
		RNN	LSTM	CNN
58.26	58.25	58.27	59.8503	45.5349
57.98	57.93	57.9375	55.2778	41.7276
61.5	61.53	61.4865	61.6866	58.4699
58.34	58.25	58.32	59.8503	45.5349
58.11	57.93	58.0975	55.2778	41.7276
61.58	61.53	61.3265	61.6866	58.4699
57.88	58.01	57.8803	60.0113	63.2916
61	61	61.045	55.3257	47.5007
59.45	59.43	60.0781	61.5911	50.5507
59.89	59.8	59.5425	59.8407	50.8514
58	58	58.2554	55.4247	56.5376
58.9	58.88	58.6707	61.6728	62.4714
59	59.02	58.9331	59.7255	54.5179
59.1	59.36	59.1622	56.0666	53.3994
57.12	57.15	57.1347	61.6354	71.3189
59.9	59.99	59.6178	59.7002	49.0664
59.5	59.35	59.4037	56.1879	59.3845
61.26	61.34	60.9056	61.5035	67.6409
57.35	57.45	57.3641	60.1922	49.0608
58.1	57.97	58.1252	56.4659	64.9688
61.1	61.06	61.085	61.8154	67.0407
58.21	57.99	57.9641	60.1922	49.0608
57.88	57.9	58.9252	56.4659	64.9688
60.94	60.7	59.775	61.8154	67.0407
56.55	56.47	57.7811	61.0532	71.6542
57.86	57.78	57.1695	55.9135	53.6723
57.16	57.29	59.2315	61.4283	46.5922
58.46	58.85	57.5482	61.0188	59.0639
55.18	55.32	56.9889	56.0912	58.9159
58.85	58.79	59.7034	61.335	64.2973
57	56.94	57.3827	61.1648	57.9369
57.97	58.22	57.4906	55.9299	65.7921
60.5	60.63	59.3856	61.2917	47.6247
57.9	57.72	57.5482	61.0188	59.0639
58.5	58.42	56.9889	56.0912	58.9159
61.23	61.26	60.7034	61.335	64.2973

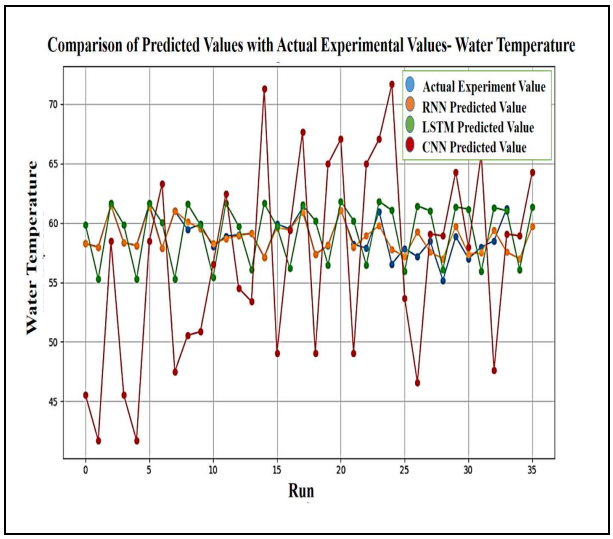

Fig. 7: Comparison of predicted vs actual values of water temperature

The performance metrics of MAE and MSE for CNN, LSTM, and RNN models in forecasting water temperature are shown in Table 8. The remarkable prediction accuracy of RNN is demonstrated by its continuously low mistakes. CNN has much larger MAE and MSE than the other models, indicating that it is less accurate for this job than LSTM, which has modest mistakes.

The line graph Fig. 7 contrasts the actual water temperature measurements with the values predicted by the CNN, LSTM, and RNN models. The tight alignment of the RNN and LSTM predictions with the actual data shows better accuracy. On the other hand, CNN predictions show a higher degree of unpredictability and notable departure from the actual values. This demonstrates that RNN and LSTM outperform CNN regarding water temperature prediction.

Table 8. ANN Performance metric of water temperature

ANN Performance Metric					
RNN		LSTM		CNN	
MAE	MSE	MAE	MSE	MAE	MSE
0.01	0	1.59	2.53	12.73	161.93
0.04	0	2.7	7.3	16.25	264.14
0.01	0	0.19	0.03	3.03	9.18
0.02	0	1.51	2.28	12.81	163.97
0.01	0	2.83	8.02	16.38	268.38
0.25	0.06	0.11	0.01	3.11	9.67
0	0	2.13	4.54	5.41	29.29
0.05	0	5.67	32.2	13.5	182.23
0.63	0.39	2.14	4.58	8.9	79.2
0.35	0.12	0.05	0	9.04	81.7
0.26	0.07	2.58	6.63	1.46	2.14
0.23	0.05	2.77	7.69	3.57	12.75
0.07	0	0.73	0.53	4.48	20.09
0.06	0	3.03	9.2	5.7	32.5
0.01	0	4.52	20.39	14.2	201.61
0.28	0.08	0.2	0.04	10.83	117.37
0.1	0.01	3.31	10.97	0.12	0.01
0.35	0.13	0.24	0.06	6.38	40.72
0.01	0	2.84	8.08	8.29	68.71
0.03	0	1.63	2.67	6.87	47.18
0.02	0	0.72	0.51	5.94	35.29
0.25	0.06	1.98	3.93	9.15	83.71
1.05	1.09	1.41	2	7.09	50.25
1.16	1.36	0.88	0.77	6.1	37.22
1.23	1.52	4.5	20.28	15.1	228.14
0.69	0.48	1.95	3.79	4.19	17.54
2.07	4.29	4.27	18.22	10.57	111.68
0.91	0.83	2.56	6.55	0.6	0.36
1.81	3.27	0.91	0.83	3.74	13.96
0.85	0.73	2.48	6.18	5.45	29.67
0.38	0.15	4.16	17.35	0.94	0.88
0.48	0.23	2.04	4.16	7.82	61.19
0.89	0.78	2.79	7.79	10.88	118.27
0.91	0.83	2.56	6.55	0.6	0.36
0.25	0.06	1.98	3.93	9.15	83.71
0.68	1.56	0.21	0.04	2.17	4.69

The RNN model outperforms the other models in terms of accuracy, as seen by its lowest average MAE of 0.16 and MSE of 0.07 in the performance metrics for water temperature. The figure 8 demonstrates the predictive accuracy of RNN, LSTM, and CNN models for water temperature in solar stills, with RNN achieving the lowest error values (MAE: 0.4454, MSE: 0.4477), followed by LSTM (MAE: 1.846, MSE: 5.598), and CNN showing the highest errors (MAE: 7.7117, MSE: 81.1913), indicating RNN's superior performance. These measurements show that the RNN model outperforms the LSTM and CNN models, making it the most dependable model for forecasting water temperature.

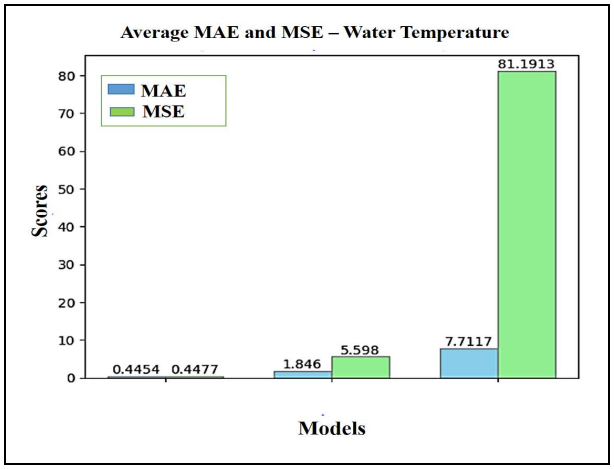

Fig. 8: MAE and MSE value measure of water temperature

4. CONCLUSION

- The RNN model consistently outperformed LSTM and CNN models in predicting solar still productivity, glass temperature, and water temperature, showing minimal error metrics (MAE and MSE), and demonstrating robust predictive capabilities.
- Solar intensity, water depth, and nanoparticle concentration were identified as critical factors influencing the thermal behavior and Productivity of the solar still, with notable differences in output between TiO_2 and CuO nanoparticles.
- TiO_2 nanoparticles were more effective than CuO in enhancing solar still Productivity, with experimental data showing Productivity varying between 0.3 to 2.75 kg/m²h.
- Actual and predicted values for Productivity, glass temperature, and water temperature were closely aligned, especially in RNN, indicating the effectiveness of the neural network approach for modeling solar still performance.
- The RNN model showed near-zero MSE in many trials, indicating its reliability, whereas LSTM demonstrated greater variability and potential for significant errors. CNN, while more stable than LSTM, had a moderate error range.
- Data from 36 trials validated the predictive power of the models under varying conditions of solar intensity, water depth, and nanoparticle concentration, confirming that higher solar intensity and nanoparticle presence generally improve productivity and temperature control.

- These findings suggest that neural networks, particularly RNNs, are promising tools for optimizing solar still designs and operating parameters, contributing to more efficient and sustainable desalination solutions.

FUNDING

This research received no specific grant from any funding agency in the public, commercial, or not-for-profit sectors.

CONFLICTS OF INTEREST

The authors declare that there is no conflict of interest.

COPYRIGHT

REFERENCE

Abdullah, A.S., Joseph, A., Kandeal, A.W., Alawee, W.H., Peng, G., Thakur, A.K. and Sharshir, S.W., Application of machine learning modeling in prediction of solar still performance: A comprehensive survey, *Results Eng.*, 21101800 (2024). https://doi.org/10.1016/j.rineng.2024.101800

Abujazar, M.S.S., Fatihah, S., Ibrahim, I.A., Kabeel, A.E. and Sharil, S., Productivity modelling of a developed inclined stepped solar still system based on actual performance and using a cascaded forward neural network model, *J. Cleaner Prod.*, 170147–159 (2018). https://doi.org/10.1016/j.jclepro.2017.09.092

Alsaiari, A.O., Moustafa, E.B., Alhumade, H., Abulkhair, H. and Elsheikh, A., A coupled artificial neural network with artificial rabbits optimizer for predicting water productivity of different designs of solar stills, *Adv. Eng. Software*, 175103315 (2023). https://doi.org/10.1016/j.advengsoft.2022.103315

Alwan, N.T., Ali, B.M., Alomar, O.R., Abdulrazzaq, N.M., Ali, O.M. and Abed, R.M., Performance of solar still units and enhancement techniques: A review investigation, *Heliyon*, 10(18), e37693 (2024). https://doi.org/10.1016/j.heliyon.2024.e37693

Elsheikh, A.H., Katekar, V.P., Muskens, O.L., Deshmukh, S.S., Elaziz, M.A. and Dabour, S.M., Utilization of LSTM neural network for water production forecasting of a stepped solar still with a corrugated absorber plate, *Process Safety Environ. Pro.*, 148273–282 (2021). https://doi.org/10.1016/j.psep.2020.09.068

Essa, F.A., Abd Elaziz, M. and Elsheikh, A.H., An enhanced productivity prediction model of active solar still using artificial neural network and Harris Hawks optimizer, *Appl. Therm. Eng.*, 170115020 (2020). https://doi.org/10.1016/j.applthermaleng.2020.115020

Hemmat Esfe, M., Esfandeh, S. and Toghraie, D., Optimization of influential geometrical parameters of single slope solar still equipped with thermoelectric system to achieve maximum desalinated water, *Energy Reports*, 75257–5268 (2021). https://doi.org/10.1016/j.egyr.2021.08.106

Mashaly, A.F. and Alazba, A.A., Neural network approach for predicting solar still production using agricultural drainage as a feedwater source, *Desalin. Water Treat.*, 57(59), 28646–28660 (2016). https://doi.org/10.1080/19443994.2016.1193770

Migaybil, H.H. and Gopaluni, B., A performance neural network model for conventional solar stills via transfer learning, *Appl. Energy*, 375124118 (2024). https://doi.org/10.1016/j.apenergy.2024.124118

Moustafa, E.B., Hammad, A.H. and Elsheikh, A.H., A new optimized artificial neural network model to predict tubular solar still's thermal efficiency and water yield, *Case Stud. Therm. Eng.*, 30101750 (2022). https://doi.org/10.1016/j.csite.2021.101750

Mustafa, M. N., Shafie, S., Wahid, M. H. and Sulaiman, Y., Preparation of TiO_2 compact layer by heat treatment of electrospun TiO_2 composite for dye-sensitized solar cells,*Thin Solid Films*, 693, 137699, (2020). https://doi.org/10.1016/j.tsf.2019.137699

Nazari, S., Bahiraei, M., Moayedi, H. and Safarzadeh, H., A proper model to predict energy efficiency, exergy efficiency, and water productivity of a solar still via optimized neural network, *J. Cleaner Prod.*, 277123232 (2020). https://doi.org/10.1016/j.jclepro.2020.123232

Senthilkumar, N., Yuvaperiyasamy, M., Deepanraj, B. and Sabari, K., Fuzzy logic-based prediction and parametric optimizing using particle swarm optimization for performance improvement in pyramid solar still, *Water Sci. Technol.*, 90(4), 1321–1337 (2024). https://doi.org/10.2166/wst.2024.277

Victor, W.J.S.D., Somasundaram, D. and Gnanadason, K., Adaptive particle swarm optimization–based deep neural network for productivity enhancement of solar still, *Environ. Sci. Pollut. Res.*, 29(17), 24802–24815 (2022). https://doi.org/10.1007/s11356-021-16840-9

Shanmugan, S., Hammoodi, K.A., Eswarlal, T., Selvaraju, P., Bendoukha, S., Barhoumi, N., Mansour, M., Refaey, H.A., Rao, M.C., Mourad, A.H.I., Fujii, M. and Elsheikh, A., A technical appraisal of solar photovoltaic-integrated single slope single basin solar still for simultaneous energy and water generation, *Case Stud. Therm. Eng.*, 54104032 (2024). https://doi.org/10.1016/j.csite.2024.104032

Sharon, H., Reddy, K.S. and Gorjian, S., Parametric investigation and yearround performance of a novel passive multi-chamber vertical solar diffusion still: Energy, exergy and enviro-economic aspects, *Solar Energy*, 211831–846 (2020). https://doi.org/10.1016/j.solener.2020.10.016

Sharshir, S.W., Elhelow, A., Kabeel, A., Hassanien, A.E., Kabeel, A.E. and Elhosseini, M., Deep neural network prediction of modified stepped double-slope solar still with a cotton wick and cobalt oxide nanofluid, *Environ. Sci. Pollut. Res.*, 29(60), 90632–90655 (2022). https://doi.org/10.1007/s11356-022-21850-2

Yuvaperiyasamy, M., Senthilkumar, N. and Deepanraj, B., Experimental and theoretical analysis of solar still with solar pond for enhancing the performance of seawater desalination, *Water Reuse*, 13(4), 620–633 (2023a). https://doi.org/10.2166/wrd.2023.102

Yuvaperiyasamy, M., Senthilkumar, N. and Deepanraj, B., Experimental investigation on the performance of a pyramid solar still for varying water depth, contaminated water temperature, and addition of circular fins, *Int. J. Renew. Energy Dev.*, 12(6), 1123–1130 (2023). https://doi.org/10.14710/ijred.2023.57327